www.ricuc.cl
DOI: 10.7764/RIC.00105.21

Revista Ingeniería de Construcción RIC
Vol 39 Nº2 2024
ISSN: 0718-5073

ENGLISH VERSION

Evaluation of the seismic performance of an educational institution using nonlinear dynamic analysis

Evaluación del desempeño sísmico de una institución educativa empleando el análisis no lineal dinámico

Paredes, A. [1] https://orcid.org/0000-0002-5944-7494*
Céspedes, J. https://orcid.org/0000-0003-1579-8388*
*Ruiz-Pico, A.**https://orcid.org/0000-0003-2638-0593*

* Universidad Católica Santo Toribio de Mogrovejo, Chiclayo – PERÚ
** Universidad Tecnológica del Perú, Chiclayo-Perú

Fecha de Recepción: 05/07/2023
Fecha de Aceptación:22/07/2024
Fecha de Publicación: 30/04/2024
PAG: 219-238

Abstract
Currently, there are a large number of old educational institutions still in operation that were built without considering earthquake-resistant criteria. These buildings, being considered essential, must maintain their operability during and after a seismic event. In this research, two two-level modules with regular plans belonging to an educational institution built in 1994 were analyzed. These modules are characterized by having a reinforced concrete frame system in the X direction and a confined masonry system in the Y direction. These modules were analyzed by applying the linear parameters of NTP E.030 and nonlinear methodologies such as the Nonlinear Dynamic Analysis (NDA), where the structures were subjected to three seismic events that occurred in Peru, which were corrected, scaled, and matched to the response spectrum using Seismosignal and Seismomatch software. ETABS software was used for modeling and following the guidelines of ASCE 41-17 and FEMA 356, the response of the seismic records in the north-south and east-west directions was evaluated, obtaining drifts and shear and displacement vs. time graphs. Based on the results, the seismic performance for both directions was obtained, considering the performance levels given by HAZUS99. It was determined that in the X direction, the performance is "Complete structural damage," and in the Y direction, it is "Slight structural damage," concluding that for this type of building, structural reinforcement in the X direction is necessary to improve performance.

Keywords: *Nonlinear dynamic analysis; seismic performance; old infrastructure; structural reinforcement; reinforced concrete frames..*

Resumen
Actualmente, existe un gran número de instituciones educativas antiguas que aún siguen en funcionamiento y han sido construidas sin tomar en cuenta criterios sismorresistentes. Estas edificaciones, por ser consideradas esenciales, deben mantener su operatividad durante y después de una solicitación sísmica. En esta investigación se analizaron dos módulos de dos niveles con plantas regulares pertenecientes a una institución educativa construida en el año 1994, los cuales se caracterizan por tener un sistema de pórticos de concreto armado en la dirección X y un sistema de albañilería confinada en la dirección Y. Estos módulos fueron analizados aplicando los parámetros lineales de la NTP E.030 y metodologías no lineales como el análisis dinámico no lineal (ADNL), donde las estructuras fueron sometidas a tres eventos sísmicos ocurridos en el Perú, las cuales fueron corregidas, escaladas y compatibilizadas con el espectro de respuesta por medio de los softwares Seismosignal y Seismomatch. Para el modelamiento se utilizó el software ETABS y, siguiendo las pautas del ASCE 41-17 y FEMA 356, se evaluó la respuesta de los registros sísmicos en las direcciones norte-sur y este-oeste, obteniéndose las derivas y gráficas de cortante y desplazamiento vs tiempo. En base a los resultados se obtuvo el desempeño sísmico para ambas direcciones, tomando en cuenta los niveles de desempeño dados por el HAZUS99, determinándose que en la dirección X presenta un desempeño de "Daños estructurales completos" y en Y de "Ligeros daños estructurales", concluyéndose que para este tipo de edificaciones es necesario un reforzamiento estructural en la dirección X para mejorar dicho desempeño.

Palabras clave: Análisis dinámico no lineal; desempeño sísmico; infraestructura antigua; reforzamiento estructural; pórticos de concreto armado.

[1] ***Corresponding author:***
Universidad Católica Santo Toribio de Mogrovejo, Chiclayo – PERÚ
Corresponding author: paredescruzariana@gmail.com

Revista Ingeniería de Construcción RIC
Vol 39 Nº2 2024
ISSN: 0718-5073

1. Introduction

It is essential to evaluate the seismic behavior of buildings (Huarca, 2022), which will depend on various aspects such as their age, structural design, type of soil, soil-structure interaction, and the seismic activity of the area (Galarza, 2019). Earthquakes produce ground oscillations that are transmitted in the form of vibrations to the structure's foundation, and simultaneously, the vibration of buildings located near the earthquake epicenter (Baba Hamed and Davenne, 2020), generating forces that can severely affect structural elements as they absorb the earthquake's input energy. These types of damages result in complex repair procedures, and in most cases, the structure may be restricted for use due to potential collapse (Pimiento et al., 2014).

Peru is one of the countries with the highest seismic frequency due to its location in the so-called Pacific Ring of Fire (Choque and Luque, 2019), characterized by an approximate extension of 40,000 km and producing earthquakes with magnitudes greater than 7Mw in the countries surrounding the Pacific Ocean (Tavera, 2014). As a result, this country has been affected by significant seismic events over the last 500 years. Cities such as Huacho, Ica, Pisco, Chincha, and Cañete have suffered damage on many occasions due to large-magnitude earthquakes. In 1996, the city of Huacho was affected by an earthquake of magnitude VIII (Jiménez et al., 2022), and in 2007, the cities from Ica to Cañete were affected by a major earthquake with intensities of VII and VI on the Mercalli scale, and a moment magnitude (Mw) of 7.9, causing significant human losses and destruction of buildings within a 250 km radius around the epicenter (Zavala et al., 2009).

Currently, there are a large number of educational institutions in this territory that were designed and built in 1994, a year when the first version of the Peruvian technical standard for earthquake-resistant design E030 was used (Ministerio de Vivienda, 2019). As a result, these structures were likely designed considering only gravity loads, without accounting for ductility and displacements, which are now considered in the E030 standard (Gonzales et al., 2020). Due to the aforementioned, there is a need to evaluate the seismic performance of buildings. Many non-linear analysis techniques and methodologies have been experimentally validated and predict structural behavior with adequate approximations (Sangucho, 2022). However, in Peru, these methods have not been incorporated into the seismic design standards, requiring reliance on foreign standards such as ASCE, FEMA, and ATC 40, which incorporate non-linear static and dynamic analysis to estimate the seismic behavior that earthquakes impose on buildings (López and Del Re Ruiz, 2008).

To determine the seismic performance of a structure, non-linear dynamic analysis or time-history analysis (NDA) is applied, which involves subjecting the structure to seismic actions that have occurred in other areas (Cumpa and Quispe, 2019). These are transformed into accelerograms that must be corrected and scaled to be applied to the building through software such as ETABS (Moller et al., 2021). This will allow for determining the seismic performance and the collapse capacity proportional to the soil acceleration caused by seismic solicitations (Baba Hamed and Davenne, 2020). Additionally, the HAZUS project is used to determine performance, which proposes four damage states associated with the maximum inter-story drift and defines them based on the structural system and the number of building levels (Díaz et al., 2022).

The aforementioned methodologies were used to determine the seismic performance of a low-rise educational institution (2 levels), built in 1994 and located in the city of Chiclayo, Peru. The standards ASCE 41-17 (ASCE/SEI 41-17, 2017), FEMA 356 (FEMA, 2000), and HAZUS99 (FEMA-HAZUS99, 2003) were applied. Furthermore, laboratory test results were used for the structural modeling. Through modeling, the seismic performance will be obtained by applying NDA, subjecting the structure to earthquakes of different magnitudes that have occurred in Peru (Blas and Sosa, 2019).

2. Materials and methods

2.1. Research Methodology

To carry out the seismic evaluation of the modules, several methodological stages were implemented. Initially, periodic visits were made to assess the current condition of the modules, and laboratory tests were conducted to determine the current characteristics of the materials. The case study was described, and the modules were modeled in ETABS software to determine the structure's weight and assess irregularities according to standard E.030. The density, axial stress, and cracking of the confined masonry walls were verified according to the masonry standard E.070 (Ministerio de Vivienda, 2006). Subsequently, accelerographic stations were defined to obtain seismic records, which were corrected and scaled in

Revista Ingeniería de Construcción RIC
Vol 39 Nº2 2024
ISSN: 0718-5073

Seismosignal and matched in Seismomatch. Additionally, nonlinear properties were assigned to the materials, plastic hinges, and selected seismic signals. Finally, the seismic performance of the modules was determined using the HAZUS99 methodology (FEMA-HAZUS99, 2003).

2.2. Current State of the Educational Institution

The structures showed problems in both structural and non-structural elements, with various pathologies indicated in (Figure 1). Through technical evaluation sheets of structural vulnerability provided by INDECI (National Institute of Civil Defense), approximate percentages were estimated for each pathology. It was found that modules A and B exhibit the highest percentage of detachments and material loss in their structural elements. In (Figure 2, it can be seen that columns are the most affected elements, as they present the highest number of pathologies.

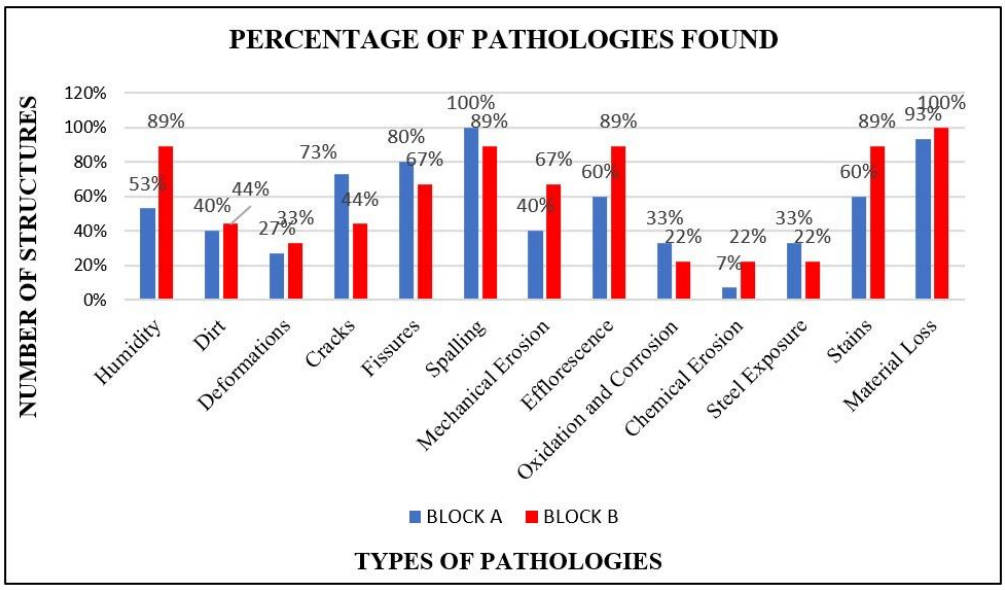

***Figure 1**. Percentage of Identified Pathologies*

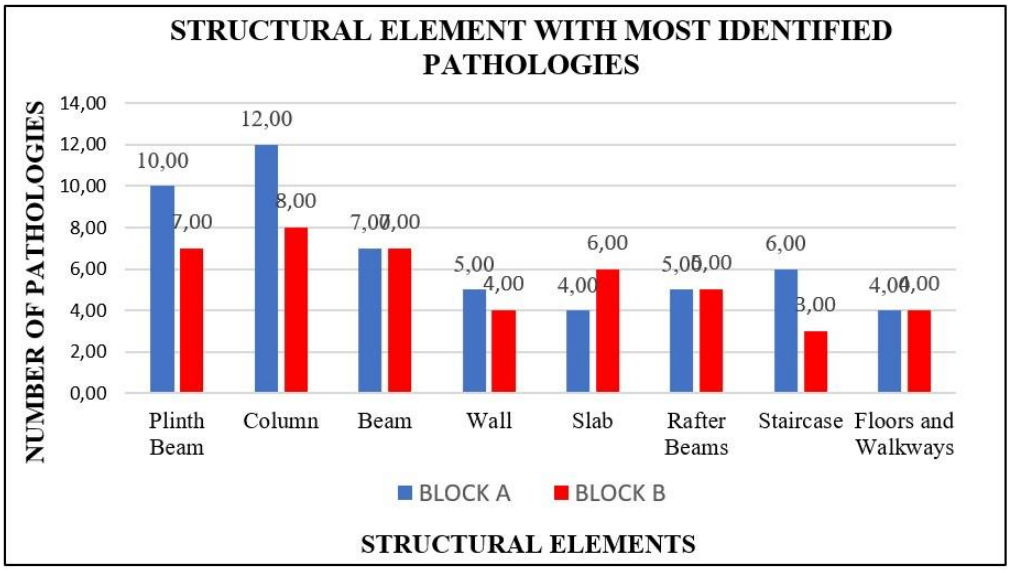

***Figure 2**. Structural Element with the Most Identified Pathologies*

Revista Ingeniería de Construcción RIC
Vol 39 Nº2 2024
ISSN: 0718-5073

2.3. Laboratory Tests

2.3.1. Extraction of Diamond Core Samples and Compression Tests

Due to the age of the educational institution, it was necessary to conduct extraction and compression tests on diamond core samples for seismic analysis, considering the standard 339.059 (Comité Técnico de Normalización, 2001). For the extraction test, 11 concrete cores were taken from the columns and beams of each module, obtaining a total of 22 samples, ensuring that the structural steel present in the modules was not affected.

For the compression test, the 22 samples were tested in a hydraulic press within 48 hours of extraction, and subsequently, the compression strength was calculated based on the length-to-diameter ratio of each core and the correction factors of the current standard. (Table 1) shows that the compression strength of the cores extracted from modules A and B does not meet the required strength for a structural element, according to standard E060 (Ministerio de Vivienda, 2009).

Table 1. *Compressive Strength of Concrete (f'c) from Diamond Cores*

N° Core	N° Floor	Element	f'c (kg/cm²) Block A	Element	f'c (kg/cm²) Block B
D-1	1st	Column	57	Column	208
D-2		Beam	141	Beam	82
D-3		Beam	131	Column	110
D-4		Column	192	Beam	120
D-5		Beam	107	Column	212
D-6		Column	135	Beam	81
D-7	2nd	Beam	124	Column	80
D-8		Column	62	Beam	166
D-9		Beam	125	Column	89
D-10		Beam	106	Beam	127
D-11		Column	72	Beam	181

2.3.2. Steel Scanner Test

Since the plans provided by the institution do not include the steel distribution, a scanner test was conducted to determine the distribution and diameters of the steel. For its execution, a Profometer PM-650 from the brand PROCEQ was used, with which scans were made on 6 columns and 10 beams of both modules. (Table 2) shows the results of some of the scans conducted, revealing steel with diameters of 5/8", 3/4", 1/2", and 1/4".

Table 2. *Results from the Reinforcement Steel Scanner Test*

N°	Element	N° Floor	Type	Scanned Margin	N° Steels	Ø	Concrete Cover (cm)
N°1	Column (C1 - 25 x 40)	1st Floor-Block B	Longitudinal	Side N°1	2	5/8	5,9 - 7,3 cm
				Side N°2	3	5/8	
			Transverse	Side N°1	13	3/8	5,4 - 7,6 cm
N°4	Beam (VX1 - 25 x 40)	1st Floor-Block B	Longitudinal	Side N°1	2	5/8	3,7 - 8,0 cm
				Side N°2	2	5/8	
			Transverse	Side N°1	37	3/8	5,4 - 10,0 cm
N°13	Column (C2 - 30 x 45)	1st Floor-Block A	Longitudinal	Side N°1	2	3/4	6,1 - 8,9 cm
				Side N°2	2	3/4	
				Side N°3	2	3/4	
			Transverse	Side N°1	12	3/8	9,1 - 10,7 cm
N°15	Beam (VY3 - 30 x 40)	1st Floor-Block A	Longitudinal	Side N°1	2	5/8	6,5 - 9,2 cm
				Side N°2	2	5/8	
				Side N°3	2	5/8	
			Transverse	Side N°1	17	3/8	4,5 - 8,8 cm

Revista Ingeniería de Construcción RIC
Vol 39 Nº2 2024
ISSN: 0718-5073

2.4. Description of the Case Study

The building studied has reinforced concrete frames in the X direction and confined masonry walls in the Y direction. Module A has a built area of 846.28 m² and has 6 rooms per level, while Module B has 633.89 m² with 4 rooms per level; both have two levels and a floor-to-floor height of 3 m. Additionally, it has seismic joints in the center of each module of 2.5 cm according to field measurements. (Table 3) shows the section of its structural elements.

Table 3. *Typical Column and Beam Sections*

Structural Elements	
Denomination	**Dimensions**
Column Nº1	0.25 x 0.40 m
Column Nº2	0.30 x 0.45 m
Column Nº3	0.25 x 0.40 m
Column Nº4	0.30 x 0.45 m
Column Nº5	0.25 x 0.25 m
Beam X1	0.25 x 0.40 m
Beam X2	0.25 x 0.40 m
Beam Y1	0.25 x 0.40 m
Beam Y2	0.30 x 0.70 m
Beam Y3 - Cantilever	0.30 x 0.40 m
Beam CH - Cantilever	0.25 x 0.20 m
Lightweight slab	e = 0.20 m

2.5. Linear modeling

ETABS software was used for the modeling of the modules; as shown in (Figure 3), each block was modeled at the seismic joint present in each of them. Then, a linear dynamic process (LDP) was performed, known in the scientific community as linear dynamic analysis, which provided a modal analysis of the structures (Collantes, 2022). After obtaining the participating masses and the vibration modes or periods (Table 4). Additionally, according to the E030 standard (Ministerio de Vivienda, 2019), the sum of effective masses must be at least 90% of the total mass, a condition that was met.

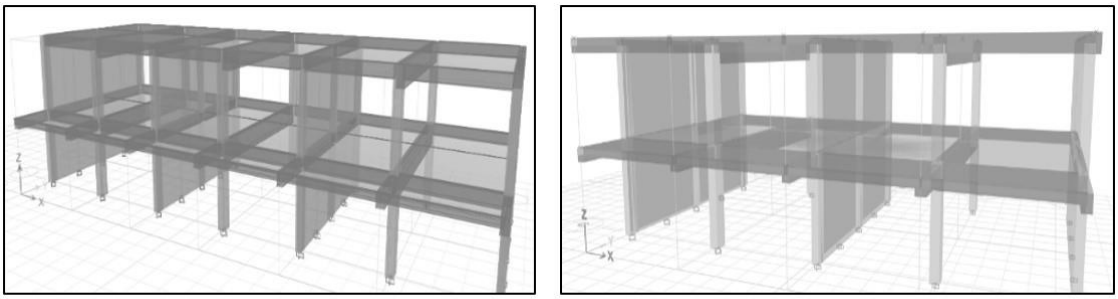

a) b)

Figure 3*. Modeling in ETABS Software: a) Module A and b) Module B*

Table 4*. Modal Results from the Numerical Model.*

Modes	Module A						
	T (Period)	Participatory Mass (%)			ΣUx (%)	ΣUy (%)	ΣRz (%)
	(sec)	Ux	Uy	Rz			
1	0.48	0.9	0	0	0.8	0.53	0
2	0.16	0.1	0	0	1	0.16	0.01
3	0.12	0	0.9	0	1	0.12	0.01
4	0.11	0	0	0.8	1	0.12	0.85
5	0.04	0	0.2	0	1	0.04	0.85

Modes	Module B						
	T (Period)	Participatory Mass (%)			ΣUx (%)	ΣUy (%)	ΣRz (%)
	(sec)	Rz	Uy	Rz			
1	0.53	0.9	0	0	0.80	0.0	0.00
2	0.16	0.1	0	0	1.00	0.0	0.00
3	0.12	0	0.9	0	1.00	0.8	0.00
4	0.12	0	0	0.9	1.00	0.8	0.85
5	0.04	0	0.2	0	1.00	0.9	0.85
6	0.03	0	0	0.2	1.00	1.0	1.00

2.6. Materials and Design Loads

(Table 5) shows the mechanical properties of concrete considered according to the E.060 standard (Ministerio de la Vivienda, 2009). The compressive strength was obtained from the average results of the compression tests on the specimens, which were used to calculate the modulus of elasticity. (Table 6) displays the mechanical parameters of masonry and steel used according to the E.070 (Ministerio de la Vivienda, 2006) and E.060 (Ministerio de la Vivienda, 2009) standards.

Table 5. *Mechanical Properties of Reinforced Concrete Used in Beams and Columns*

Properties of Reinforced Concrete					
Average Compressive Strength					Unit Weight (kg/cm^2)
Module	N° Floor	Element	F'c (kg/cm^2)	Modulus of Elasticity (kg/cm^2)	
A	1st	Columns and Beams	127.17	169155	2400
	2nd	Columns and Beams	97.80	148341	
B	1st	Columns and Beams	134.33	173851	2400
	2nd	Columns and Beams	128.60	170103	

Table 6. *Characteristics of Steel and Masonry*

Material	Properties	
Reinforcing Steel	Unit Weight	7850 kg/m^3
	Modulus of Elasticity	2000000 kg/cm^2
	Yield Strength (fy)	4200 kg/cm^2
Masonry	Unit Weight of Solid Masonry Units	1800 kg/cm^3
	Shear Strength in Wall Testing (v'm)	8.1 kg/cm^2
	Axial Compression Strength (f'm)	65 kg/cm^2
	Modulus of Elasticity (Em=500 x f'm)	32500 kg/cm^2
	Poisson's modulus μ	0.25

(Table 7) shows the magnitudes of live and dead loads for modeling. These loads correspond to the E.020 load standard (Ministerio de Vivienda, 2006).

Table 7. *Loads Used in Modules A and B*

Parameter	Live Load	Dead Load
Classrooms	250 kg/m^2	
Corridors	400 kg/m^2	
Lightened Slab Thickness = 20 cm		350 kg/m^2
Finishes		100 kg/m^2
Parapet		202.50 kg/m
Sill 1		263.25 kg/m
Sill 2		416.14 kg/m

Revista Ingeniería de Construcción RIC
Vol 39 Nº2 2024
ISSN: 0718-5073

2.7. Linear Analysis

2.7.1 Seismic Parameters

The E030 standard (Ministerio de Vivienda, 2019) was used to define the seismic parameters (Table 8). Additionally, irregularities in plan and elevation were checked; the result was that both modules are regular in both cases.

Table 8. *Loads Used in Modules A and B*

Seismic Parameters	Module A		Module B	
	X-X	Y-Y	X-X	Y-Y
Zone Type	4	4	4	4
Zone Factor (Z)	0.45	0.45	0.45	0.45
Soil Type	S3	S3	S3	S3
Soil Factor (S)	1.1	1.1	1.1	1.1
Predominant Period Tp - Sec	1	1	1	1
Local Period TL - Sec	1.6	1.6	1.6	1.6
Fundamental Period T - Sec	0.487	0.126	0.53	0.13
Seismic Amplification Factor (C)	2.5	2.5	2.5	2.5
Category	A	A	A	A
Usage Factor (U)	1.5	1.5	1.5	1.5
Irregularity Factor in Plan (Ip)	1	1	1	1
Irregularity Factor in Height (Ia)	1	1	1	1
Basic Reduction Coefficient (Ro)	8	3	8	3
Reduction Coefficient (R)	8	3	8	3

2.7.2 Structural Weight

The structural weight of the modules was obtained from the ETABS software; for this, a distribution of 100% dead load and 50% live load was considered, as it is a Category A building (Ministerio de Vivienda, 2019). (Table 9) presents the weight of both modules.

Table 9*. Weight of Modules A and B*

Mass - Module A			Mass - Module B	
Level	Mass X	Mass Y	Mass X	Mass Y
	Tonf-s²/m	Tonf-s²/m	Tonf-s²/m	Tonf-s²/m
Level 2	13.86	13.86	11.44	11.44
Level 1	23.65	23.65	16.27	16.27
Total	37.51	37.51	27.71	27.71
Weight (Ton)	368.02 Ton	368.02 Ton	271.88 Ton	271.88 Ton

2.7.3 Shear Force at the Base

With the weight and seismic parameters already defined, a linear static analysis was performed, where the total shear force at the base of the structure was calculated using (Equation 1) from the E030 standard (Ministerio de Vivienda, 2019).

$$V_{Basal} = \frac{Z * U * C * S}{R} * P \quad \textbf{(1)}$$

Where,

Z= Zone Factor
U= Usage Factor
C= Seismic Amplification Factor
S= Soil Factor

Revista Ingeniería de Construcción RIC
Vol 39 Nº2 2024
ISSN: 0718-5073

R= Basic Reduction Coefficient
P= Structure weight

2.7.4 Response Spectrum

A spectral modal dynamic analysis was performed, where the spectral acceleration was calculated based on seismic parameters according to the E030 standard (Ministerio de Vivienda, 2019). (Figure 4) shows the response spectra for the X and Y directions. It is noted that for the same seismic zoning, the maximum acceleration is directly proportional to the period and magnitude of the acceleration and the type of soil. Therefore, it is important to consider that soft soils (S3) will result in greater responses for the building (Collantes, 2022).

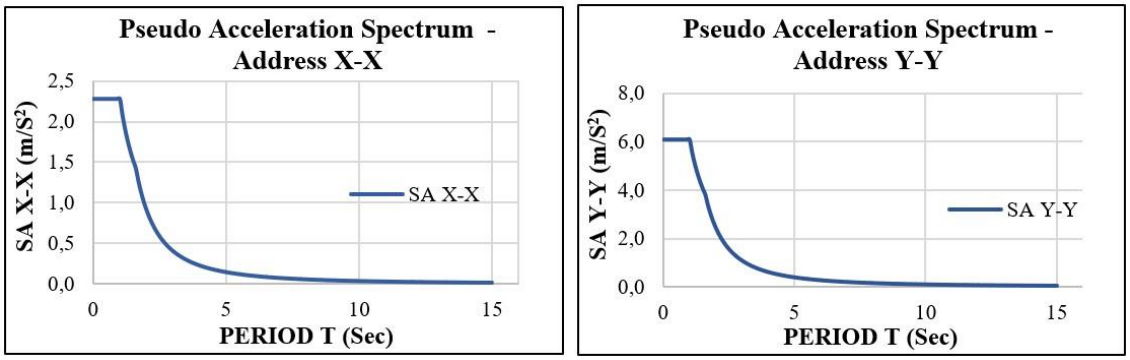

Figure 4. *Response Spectrum in the X and Y Directions*

2.8. Confined Masonry Walls

2.8.1 Wall Density

According to the masonry standard E070 (Ministerio de Vivienda, 2006), there must be a minimum density of load-bearing walls in the floor area of a building; for this purpose, (Equation 2) provided by the standard was applied.

$$\frac{\sum L \cdot t}{A_p} \geq \frac{Z \cdot U \cdot S \cdot N}{56} \quad \textbf{(2)}$$

Where,
L= Total length of wall (m)
t= Wall Thickness (m)
Ap= Typical Plant Area (m2)

2.8.2 Maximum Axial Stress

The maximum axial stress was verified according to the masonry standard E070 (Ministerio de Vivienda, 2006), where a maximum service gravity load (Pm) representing 100% dead load and 100% live load was considered.

2.8.3 Crack Control

The cracking of the walls was verified according to the E070 standard (Ministerio de Vivienda, 2006), where a gravity load (Pg) representing 100% dead load and 50% live load was considered.

2.9. Nonlinear Dynamic Analysis – Time History

2.9.1 Seismic Records

Eight pairs of seismic records were selected, following the recommendations indicated by the 2018 FEMA standard. These records were selected from the accelerographic stations of Peru provided by the Center for Seismic Engineering Observation (CISMID), considering their magnitude and the type of soil of the station that recorded them. (Table 10) shows the selected seismic records.

2.9.2 Scaling of Seismic Records

The scaling of the earthquakes was carried out following the procedures of (Álvarez et al., 2022), defining the areas where large magnitude earthquakes are generated and selecting earthquakes with nearby coordinates where historical earthquakes occurred. These seismic signals were corrected for baseline using the SeismoSignal software (SeismoSoft, 2020). The corrected accelerograms were scaled for a design earthquake in the EO and NS directions, considering the maximum absolute value of acceleration for each direction with which the scaling factor was calculated based on the already defined seismic parameters. Finally, the Seismomatch software was used to perform the spectral adjustment of the scaled earthquakes with the response spectrum obtained from the E.030 standard (Ministerio de Vivienda, 2019). (Figure 5) and (Figure 6) shows some of the scaled accelerograms.

Revista Ingeniería de Construcción RIC
Vol 39 Nº2 2024
ISSN: 0718-5073

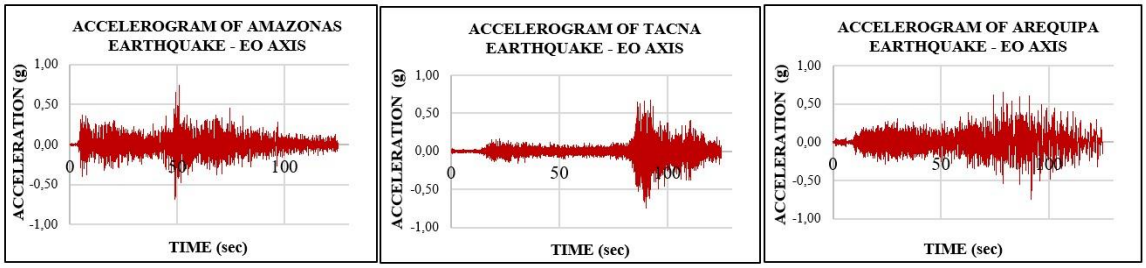

***Figure 5**. Scaled Accelerograms in the EO Direction*

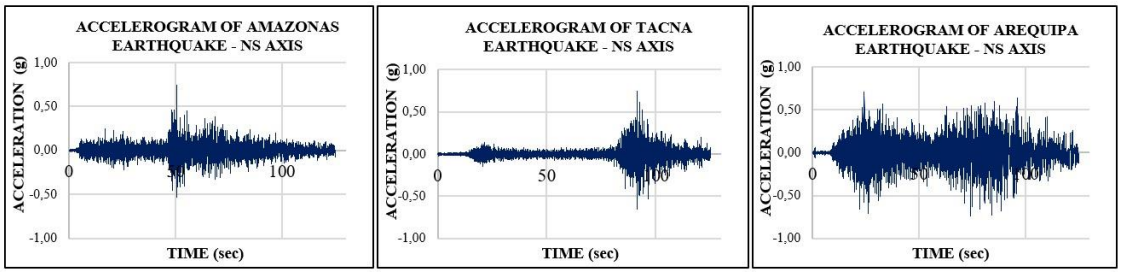

***Figure 6**. Scaled Accelerograms in the NS Direction*

***Table 10.** Selected Accelerographic Stations*

Station	Name	Magnitude	Max Accelerations			Depth (Km)
			EO	NS	UD	
Nº1 IQU001	90 km East of Sta. María De Nieva, Condorcanqui - Amazonas	6.8 M	5.12	6.72	5.98	139
Nº2 TAC004	689 km South-SE of Tacna, Tacna - Tacna	6.8 M	3.36	4.56	2.74	244
Nº3 CAL001	56 km South of Lomas, Arequipa	6.8 Mw	4.92	5.23	2.32	48
Nº4 AQP-003	20 km NE of Ayaviri, Melgar - Puno	6.9 M	12.8	12.44	10.91	240
Nª5 CAL 001	Pisco Earthquake	7 ML	101.03	95.76	31.63	40
Nº6 CAL 001	70 km SE of Lagunas, Alto Amazonas - Loreto	7.2 ML	15.06	14.21	7.36	141
Nª7 CAL 001	98 km East of Sta. María De Nieva, Condorcanqui - Amazonas	7.5 M	7.27	6.28	3.08	131
Nª8 IQU 001	1114 km NW of Pastaza, Alto Amazonas - Loreto	7.7 ML	10.63	10.35	7.83	139

2.9.3 Seismic Records

The software Seismomatch was used to evaluate the accelerograms compatible with the response spectrum, from which three were selected as indicated in the E030 standard (NTP Ministerio de Vivienda, 2019). (Figure 7) presents the response spectra of the selected earthquakes for both directions.

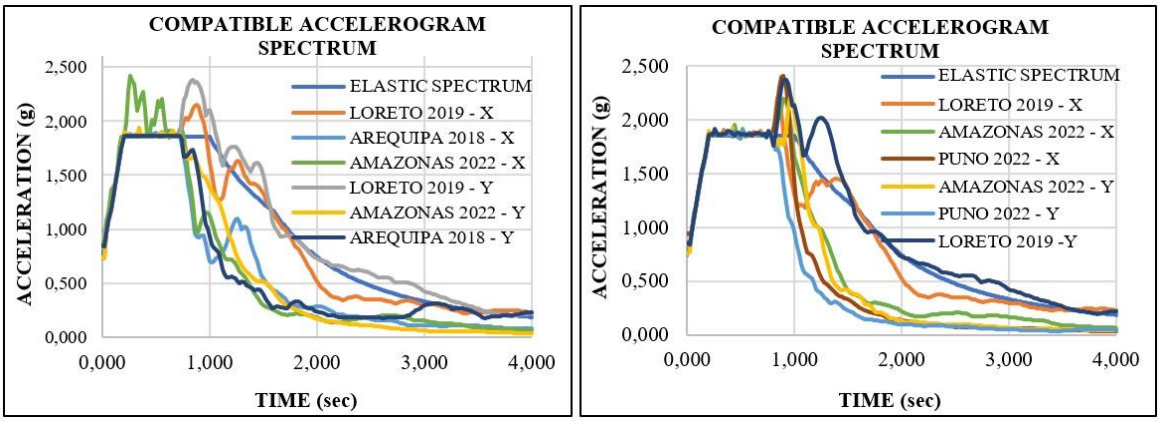

Figure 7*. Selected Response Spectra: a) Module A and b) Module B*

2.10. Nonlinear Modeling

For nonlinear analysis, the ETABS software was used following the criteria of FEMA 356 (FEMA, 2000), in which nonlinear properties were assigned to the materials; among these, we have the Kent-Park model assigned to the reinforcing steel and the Mander model assigned to the concrete, detailed in (Guohua et al., 2020). (Figure 8) shows the stress-strain graphs of the aforementioned models. To evaluate the damage level of the structure, plastic hinges were placed according to the ASCE standard (ASCE, 2017); these are located at 0% and 100% of the columns and beams. For the modeling of the confined masonry walls, the procedure of (Gonzales et al., 2020) was applied, which consists of modeling the wall as a concrete frame element where a shear hinge located at 50% of its total height with the properties of the capacity curve taken from this research will be assigned. These are shown in (Figure 9).

In the modeling, 3 accelerograms were selected and entered for the east-west and north-south directions in the Time History function of ETABS, where a gravity case was also created, with a distribution of 100% dead load and 50% live load, which served as an initial condition for each seismic record analyzed.

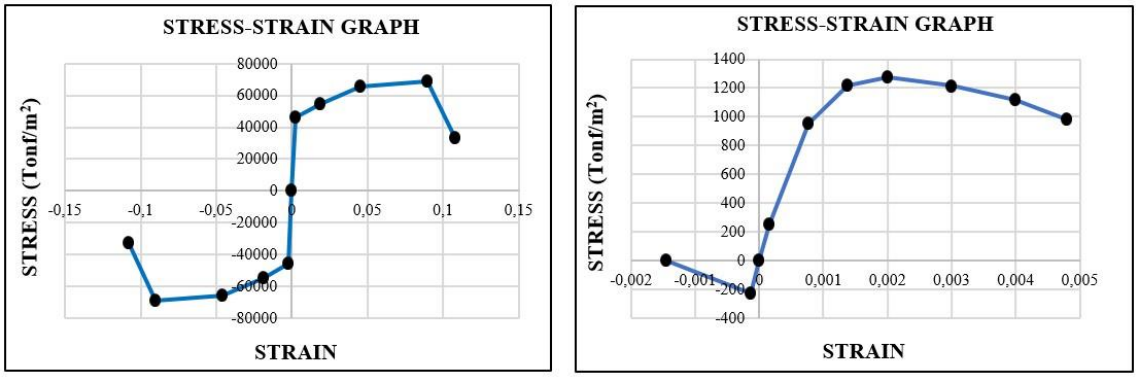

Figure 8. *Stress-Strain Diagram: a) Steel and b) Concrete of 127.17 kg/cm²*

Revista Ingeniería de Construcción RIC
Vol 39 Nº2 2024
ISSN: 0718-5073

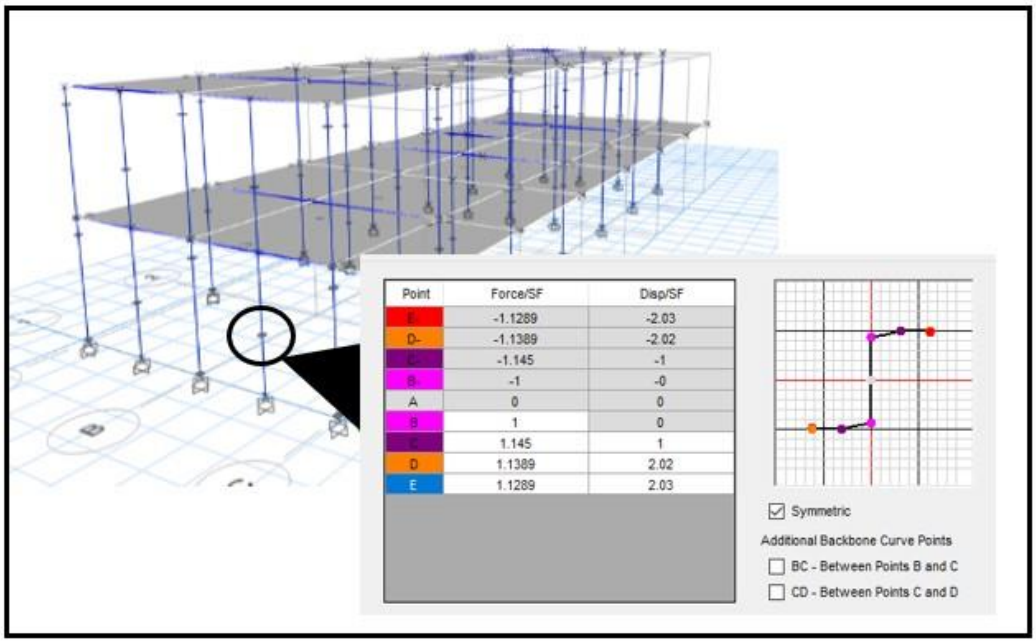

Figure 9. *Nonlinear Parameters Used for Masonry Walls*

2.11. Seismic Performance

To determine the seismic performance, the procedure used by (Díaz et al., 2022) was applied, where 4 damage states that structures can suffer are evaluated through (Figure 10) according to HAZUS99 (FEMA-HAZUS99, 2003).

Table 5.9b Structural Fragility Curve Parameters – Moderate Code Seismic Design Level

Building Properties			Interstory Drift at Threshold of Damage State			
Type	Height (inches)					
	Roof	Modal	Slight	Moderate	Extensive	Complete
S5L S5M S5H						
C1L	240	180	0.0050	0.0087	0.0233	0.0600
C1M	600	450	0.0033	0.0058	0.0156	0.0400
C1H	1440	864	0.0025	0.0043	0.0117	0.0300

Figure 10. *Damage States According to FEMA – HAZUS 99.*

3. Results

3.1 Linear Analysis

3.1.1 Base Shear

The calculation of the static base shear was based on the product of the seismic coefficients in X and Y and the seismic weight; the coefficients were 0.23 and 0.62 for X and Y, respectively; the seismic weight was 368 tons for module A and 271.9 tons for module B. For the dynamic shear, the ETABS software was used. According to the aforementioned standard, the dynamic shear must be greater than or equal to 80% of the static shear for regular structures, a condition that is met in both modules. (Table 11) and (Table 12) shows the base shears for both directions.

Table 11. *Static Base Shear*

Block	Module A		Module B	
AXIS	X-X	Y-Y	X-X	Y-Y
ZUCS/R	0.23	0.62	0.23	0.62
P (Ton)	368.02	368.02	271.88	271.88
V(Ton)	85.39	227.71	63.08	168.23

Table 12. *Dynamic Base Shear of Modules A and B*

Axis/Module	Module A	Module B
X-X	74.90 Ton	55.14 Ton
Y-Y	196.03 Ton	144.97 Ton

3.1.2 Maximum Lateral Displacements

To obtain the maximum displacements, a displacement factor of 6 in the X direction and a factor of 2.25 for Y was used in the ETABS software, which is the result of 75% of the reduction coefficient (R) for regular structures according to NTP E.030. (Table 13) shows the maximum displacements for each module. (Table 14) shows that the calculated seismic joint is greater than the actual seismic joint, which could cause a pounding problem.

Table 13. *Maximum Displacements of Modules A and B*

Type of Analysis	N° Floor	Axis	Module	Max. Displacement (m)	Displacement (cm)
Static Linear	2	X-X	A	0.14	14.12
	1			0.06	6.43
	2		B	0.14	14.12
	1			0.06	6.43
	2	Y-Y	A	0.01	0.98
	1			0.00	0.43
	2		B	0.01	0.96
	1			0.00	0.42
Dynamic Linear	2	X-X	A	0.11	10.78
	1			0.05	5.00
	2		B	0.13	12.51
	1			0.06	5.65
	2	Y-Y	A	0.01	0.86
	1			0.00	0.37
	2		B	0.01	0.85
	1			0.00	0.36

Table 14*. Joint Seismic Verification*

Type of Analysis	Module	Axis	Joint (cm)	Actual Joint (cm)
Static Linear	A	X-X	4	2.5
	B		4	2.5
Dynamic Linear	A		4	2.5
	B		4	2.5

Revista Ingeniería de Construcción RIC
Vol 39 Nº2 2024
ISSN: 0718-5073

(Table 15) shows the drifts, where for reinforced concrete elements (X direction) they should not exceed the value of 0.007 and for masonry (Y direction) the value of 0.005 according to NTP E.030; however, it is noted that in the X direction, the drifts in both modules do not meet the requirements, which presents a design issue in the structures.

***Table 15**. Drift Verification of Modules A and B*

Type of Analysis	N° Floor	Axis	Block	Drift	Max Drift	Verification
Static Linear	2	X-X	A	0.021	< 0.007	Does Not Comply
	1			0.018	< 0.007	Does Not Comply
	2		B	0.025	< 0.007	Does Not Comply
	1			0.021	< 0.007	Does Not Comply
	2	Y-Y	A	0.001	< 0.005	Complies
	1			0.001	< 0.005	Complies
	2		B	0.001	< 0.005	Complies
	1			0.001	< 0.005	Complies
Dynamic Linear	2	X-X	A	0.019	< 0.007	Does Not Comply
	1			0.016	< 0.007	Does Not Comply
	2		B	0.023	< 0.007	Does Not Comply
	1			0.018	< 0.007	Does Not Comply
	2	Y-Y	A	0.001	< 0.005	Complies
	1			0.001	< 0.005	Complies
	2		B	0.001	< 0.005	Complies
	1			0.001	< 0.005	Complies

3.1.3 Confined Masonry Walls

Applying the procedures of NTP E.070, three verifications were performed in the Y direction: load-bearing wall density (Table 16), maximum axial stress (Table 17), and cracking control (Table 18). The results between the two modules vary because they have different floor areas, and module A has four masonry walls, while module B has only three walls.

***Table 16**. Wall Density Verification*

WALL DENSITY			
Block	**ΣL.t/Ap**	**ZUSN/ 56**	**Compliance**
A	0.043	0.027	Yes
B	0.038	0.027	Yes

***Table 17**. Maximum Axial Stress Verification*

Revista Ingeniería de Construcción RIC
Vol 39 Nº2 2024
ISSN: 0718-5073

MAXIMUM AXIAL LOAD							
Block	**Level**	**Wall**	**σm kg/cm²**	**$\sigma m \leq 0.2 * f'm \left[1-\left(\frac{h}{35*t}\right)^2\right]$**		**$\sigma m \leq 0.15 * f'm$**	
A	1st	M Y-1	2.72	11.47	Yes	9.75	Yes
		M Y-2	3.99	11.47	Yes	9.75	Yes
		M Y-3	3.99	11.47	Yes	9.75	Yes
		M Y-4	2.67	11.47	Yes	9.75	Yes
	2nd	M Y-1	1.15	11.47	Yes	9.75	Yes
		M Y-2	1.62	11.47	Yes	9.75	Yes
		M Y-3	1.62	11.47	Yes	9.75	Yes
B	1st	M Y-4	1.15	11.47	Yes	9.75	Yes
		M Y-1	2.85	11.47	Yes	9.75	Yes
		M Y-2	4.23	11.47	Yes	9.75	Yes
	2nd	M Y-3	2.81	11.47	Yes	9.75	Yes
		M Y-1	1.29	11.47	Yes	9.75	Yes
		M Y-2	1.87	11.47	Yes	9.75	Yes
		M Y-3	1.29	11.47	Yes	9.75	Yes

Table 18. *Wall Cracking Verification*

CRACK CONTROL					
Block	**Floor**	**Wall**	**Ve (Ton)**	**0.55*Vm**	**Verification**
A	1st	M Y-1	27.29	48.93	No Cracking
		M Y-2	24.37	51.58	No Cracking
		M Y-3	24.26	51.58	No Cracking
		M Y-4	26.95	48.83	No Cracking
	2nd	M Y-1	15.09	45.47	No Cracking
		M Y-2	13.48	46.5	No Cracking
		M Y-3	13.44	46.5	No Cracking
		M Y-4	14.96	45.48	No Cracking
B	1st	M Y-1	26.39	49.24	No Cracking
		M Y-2	22.76	52.13	No Cracking
		M Y-3	26.07	49.14	No Cracking
	2nd	M Y-1	15.63	45.79	No Cracking
		M Y-2	13.48	47.05	No Cracking
		M Y-3	15.52	45.79	No Cracking

3.2. Nonlinear Dynamic Analysis

An aerial trimming of the seismic records had to be performed. It is recommended to trim 5% and 95% of the total data from each accelerogram. Due to the extensive computational process involved, only 60 seconds were analyzed for each record, using a time interval of 0.005 seconds.

Using ETABS software, the base shear vs. time (Figure 11) and displacements vs. time (Figure 12) were obtained. From the three earthquakes analyzed for module A, it was found that the Loreto earthquake (2019) generated the highest shear force in the structure, with a value of 222.15 tons at a time of 7.98 seconds and a maximum displacement of 30.9 cm at a time of 12 seconds in the X direction, while in the Y direction, the Arequipa earthquake (2018) generated the highest shear force with a value of 397.092 tons at a time of 41.89 seconds and a maximum displacement of 1.12 cm at a time of 41.89 seconds. In module B, it was found that the Loreto earthquake (2019) in the X direction generated a maximum shear force of 157.19 tons at a time of 7.97 seconds and a maximum displacement of 28.79 cm at a time of 8.19 seconds, while in the Y direction, it generated a shear force of 291.92 tons at a time of 28.78 seconds and a maximum displacement of 1.06 cm at a time of 28.79 seconds.

The drifts for each level were also obtained (Table 19), showing that for module A, the Loreto earthquake (2019) generated maximum drifts in both directions and for module B in the X direction; however, in the Y axis, maximum drifts were generated by the Amazonas earthquake (2022). Additionally, the drifts in the Y axis complied with the standard, but in the X axis, they were unsatisfactory as none complied with the maximum drift allowed by NTP E.030.

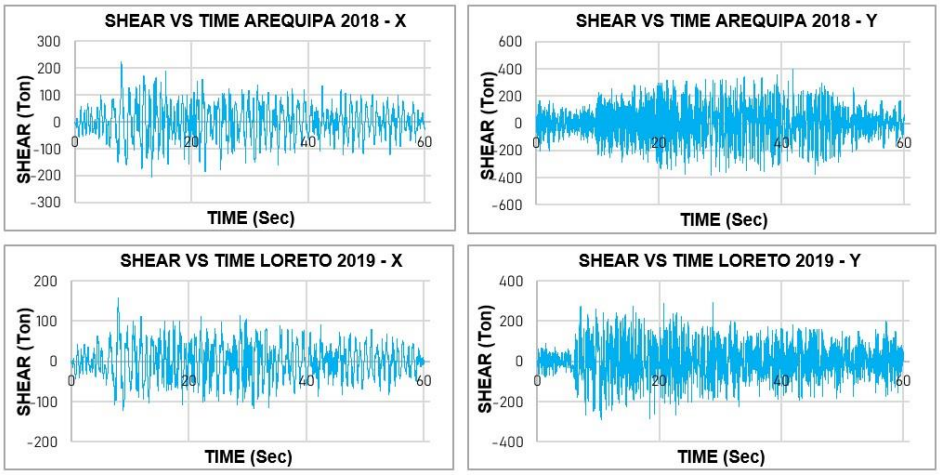

Figure 11. *Shear vs Time Graphs*

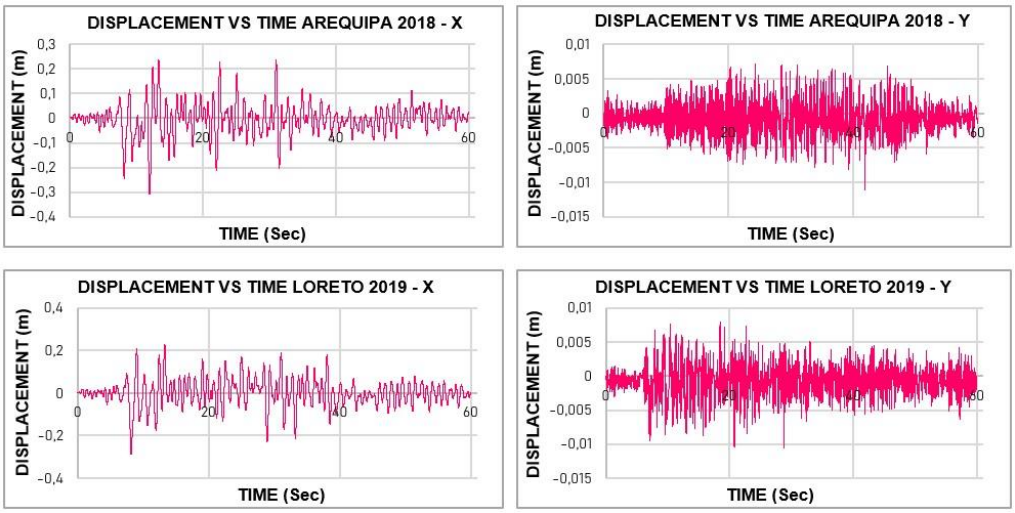

Figure 12. *Displacement vs Time Graphs*

Table 19*. NDA Drift Verification*

Revista Ingeniería de Construcción RIC
Vol 39 Nº2 2024
ISSN: 0718-5073

Block	Floor	Axis	Earthquake	Drift	Max Drift	Verification
A	2	X	Amazonas 2022	0.035	< 0.007	No
	1			0.018	< 0.007	No
	2		Arequipa 2018	0.045	< 0.007	No
	1			0.020	< 0.007	No
	2		Loreto 2019	0.056	< 0.007	No
	1			0.026	< 0.007	No
	2	Y	Amazonas 2022	0.001	< 0.005	Yes
	1			0.001	< 0.005	Yes
	2		Arequipa 2018	0.001	< 0.005	Yes
	1			0.001	< 0.005	Yes
	2		Loreto 2019	0.001	< 0.005	Yes
	1			0.002	< 0.005	Yes
B	2	X	Amazonas 2022	0.056	< 0.007	No
	1			0.029	< 0.007	No
	2		Puno 2022	0.040	< 0.007	No
	1			0.019	< 0.007	No
	2		Loreto 2019	0.052	< 0.007	No
	1			0.026	< 0.007	No
	2	Y	Amazonas 2022	0.001	< 0.005	Yes
	1			0.001	< 0.005	Yes
	2		Puno 2022	0.001	< 0.005	Yes
	1			0.002	< 0.005	Yes
	2		Loreto 2019	0.001	< 0.005	Yes
	1			0.002	< 0.005	Yes

3.3. Sysmic Performance

The seismic performance was determined by applying the HAZUS99 standard (Figure 10), which was determined based on inter-story drifts. (Table 20) shows that both modules exhibit slight structural damage in the Y direction; however, in the X axis, they show complete structural damage, which means the total collapse of the structures.

***Table 20**. Seismic Performance of Modules A and B*

Block	Axis	Earthquake	Drift	Damage State
A	X-X	Amazonas 2022	0.035	Extensive Structural Damage
		Arequipa 2018	0.045	Complete Structural Damage
		Loreto 2019	0.056	Complete Structural Damage
B	Y-Y	Amazonas 2022	0.001	Minor Structural Damage
		Arequipa 2018	0.001	Minor Structural Damage
		Loreto 2019	0.001	Minor Structural Damage
A	X-X	Amazonas 2022	0.056	Extensive Structural Damage
		Puno 2022	0.040	Complete Structural Damage
		Loreto 2019	0.052	Complete Structural Damage
B	Y-Y	Amazonas 2022	0.001	Minor Structural Damage
		Puno 2022	0.001	Minor Structural Damage
		Loreto 2019	0.001	Minor Structural Damage

4. Discussion

4.1 Ranking of change orders factors

The educational institution can be said to have deficiencies because it was built under an older version of NTP E.030, which did not include the criteria currently in use. This has impacted various situations, including the behavior of buildings that collapsed during the Ecuador earthquake in 2016. (Castañeda and Bravo, 2017) highlight this issue, noting that civil engineers at that time lacked standardized procedures to collect information on damaged buildings, which hindered learning and the improvement of existing regulations. According to (Condori and Vilca, 2022), numerous earthquakes of various

Revista Ingeniería de Construcción RIC
Vol 39 Nº2 2024
ISSN: 0718-5073

magnitudes have historically damaged structures whose designs were not based on the current Peruvian seismic technical standard E.030, making them more vulnerable to high-intensity earthquakes and significantly increasing the rigidity requirements.

In the linear analysis performed on modules A and B, it was determined that they did not meet all the parameters established for an essential building as given by (Ministerio de Vivienda, 2019). This is because the drifts in the X-axis exceeded the maximum drift of 0.007, and the calculated seismic joint was greater than the current seismic joint. According to (Mohammed et al., 2013), this causes pounding that increases damage to structural components to the point of causing the structure to collapse. Similar results regarding drifts were obtained in the research by (Gonzales et al., 2020), who analyzed an old essential reinforced concrete building with confined masonry, finding that the drifts in both directions exceeded 0.5%, the limit according to the Peruvian standard. However, one way to solve this issue is by including T-columns, which help control displacements in the most unfavorable direction; an example is the I.E. San Carlos Monsefú, an optimized structure by Greta Llontop in 2023, which met the drifts required by the E.030 standard.

Similarly, (Firoj et al., 2022) suggested that results can be optimized by improving stiffness in the most unfavorable direction, reducing the fundamental period of vibration, and evaluating the flexible behavior of the soil. Moreover, (Lu and Phillips, 2022) demonstrate that seismic retrofitting methodologies that preserve the fundamental period in low-rise buildings reduce normalized input forces and attenuate higher frequency responses, thus reducing displacement responses.

Regarding base shears, module A shows a higher shear compared to module B, with a maximum value of 85.39 tons in the X-axis and 227.71 tons in the Y-axis. This is because module A has a larger floor area and thus greater structural weight compared to module B. According to (Firoj et al., 2022), base shear depends on the self-weight of the structure; as the self-weight of the model increases, the base shear increases; an example is the institution evaluated by engineer Christian Asmat, who achieved a static base shear in X and Y of 267 tons. This is because the weight of the structure reaches 905 tons. (Reza et al., 2022) made a comparative table of the variation of shears in different concrete structures, as shown in (Table 21). This table shows that the base shears of modules A and B differ slightly due to their different floor areas, unlike buildings 1 and 2, where the base shear mainly differs due to the number of floors in each building.

***Table 21**. Base Shear Comparison*

Building	Number of Levels	Base Shear (Ton)
Module A	2	222.15
Module B	2	157.19
Building 1	3	295.69
Building 2	6	334.48

From the nonlinear dynamic analysis, it was found that, for module A, the maximum base shear in the X direction is 222.15 tons with a displacement of 0.31 m; and in the Y direction, the shear is 397.092 tons with a displacement of 0.11 m. For module B, in the X direction, the shear is 157.19 tons with a displacement of 0.29 m; and in the Y direction, the shear is 291.92 tons with a displacement of 0.11 m. The variation in these results is due to the fact that the X axis has a reinforced concrete frame system, resulting in lower shear and greater displacement, while the Y axis has a confined masonry structural system, offering higher shear and stiffness but less ductility. These findings are corroborated by the research of (Cienfuegos, 2022) at I.E. 10202 "Virgen de la Paz" in Pacora, where the maximum base shears were 279.94 tons in the X axis and 396.63 tons in the Y axis during the Pisco earthquake; these results are relevant because they refer to a building with the same structural system as the one evaluated in the present research.

According to (Pérez and Torres, 2022) and the NTP E030 of 2019, an essential building must have life safety performance during a maximum earthquake, similar to the state of moderate structural damage (FEMA-HAZUS99, 2003). The results show that the X axis does not meet this condition, as it presents a performance of complete structural damage. However, each building has its own seismic behavior, influenced by materials, construction process, and structural design. (Álvarez et al., 2022) demonstrated that low-rise reinforced masonry houses can achieve immediate occupancy performance, allowing their use after an earthquake.

The educational institution presents a deficient structural design, as both modules have low stiffness in the X direction due to the section of their columns, steel quantities, low compressive strength, and the absence of rigid elements to control displacements (Marín, 2020). If a severe seismic event were to occur, the X axis would collapse due to the loss of stiffness of its structural elements. This structural response is realistic, as, according to (Baris et al., 2022), nonlinear analysis is more effective in evaluating the seismic performance of buildings with a dual system of reinforced concrete and masonry. This assertion is based on a seismic performance evaluation applied to a historical building in Istanbul. For this reason, these results are of great importance.

5. Conclusion

From the linear analysis, it can be concluded that the structures did not meet the drift requirements in the X direction, as Module A exhibited a maximum drift of 0.0217 in the X axis and Module B exhibited a drift of 0.0256, thereby exceeding the maximum limit of 0.007 for reinforced concrete structures as specified by the E.030 standard. On the other hand, they complied with the irregularities and the verification of masonry load-bearing walls according to the E.070 standard, and therefore do not exhibit cracking and buckling failures (Table 16), (Table 17), and (Table 18).

It is concluded that the Loreto earthquake (2019) generated the maximum shear forces and displacements in both modules, as it had the greatest magnitude of the three selected records. In Module A, the maximum shear force was 222.15 tons with a displacement of 30.9 m in the X direction, while in the Y direction, the shear force was 394.66 tons with a displacement of 0.94 m.

In Module A, the Loreto earthquake (2019) generated the maximum drifts with a value of 0.0564 in the X direction and 0.0016 in the Y direction, while in Module B, the Amazonas earthquake (2022) generated the maximum drifts with a value of 0.0563 in the X direction and 0.0013 in the Y direction, due to their intensities of 6.8 and 7.7, considered as strong and very strong earthquakes according to the Mercalli scale.

According to the HAZUS99 method, it was found that when applying the three accelerograms, the modules collapse in the X direction with a seismic performance of "Complete structural damage," indicating the failure of all their structural elements, while in the Y direction, they maintain "Slight structural damage."

It is concluded that the application of nonlinear dynamic analysis is beneficial in evaluating the structural performance of buildings, as it allows for a more accurate determination of the behavior of buildings under possible future seismic demands.

7. Referencias

Álvarez Deulofeu, E. R.; Lora Alonso, F.; López Chang, S. (2022). *Proceso de diseño sismorresistente de edificios de viviendas de mampostería reforzada para zonas de alta peligrosidad sísmica, 74(566). Informes de la Construcción, e445. https://doi.org/10.3989/ic.85554.*

American Society of Civil Engineers. (2017). *ASCE/SEI, 41-17, Seismic Evaluation and Retrofit of Existing Buildings. United States of America.*

Asmat, C. (2016). *Disposiciones sísmicas de diseño y análisis en base a desempeño aplicables a edificaciones de concreto armado. Pontifica Universidad Católica del Perú.*

Baba Hamed, F., & Davenne, L. (2020). *Effect of the viscous damping on the seismic response of Low-rise RC frame building, (96). Revista Facultad de Ingenieria, 32-43. https://doi.org/10.17533/udea.redin.20191045*

Baris, G.; Atakan, M.; Turgay, C.; Baris, S.; Cemil, A. (2022). *Seismic performance assessment of a historical masonry-infilled RC building located in the historical peninsula of Istanbul (1940s), (45). Structures, 951-968. https://doi.org/10.1016/j.istruc.2022.09.074.*

Blas, J.; Sosa, E. (2019). *Evaluación del desempeño sísmico bajo el método de análisis estático no lineal Pushover, caso puente Riecito ubicado en el distrito de Bellavista – Piura [Universidad Ricardo Palma].https://repositorio.urp.edu.pe/bitstream/handle/ 20.500.14138/2634/T030_71129000-T.pdf?sequence=1&isAllowed=y*

Castañeda, Á.; Bravo, Y. (2017). *Overview of the Structural Behavior of Columns, Beams, Floor Slabs and Buildings during the Earthquake of 2016 in Ecuador, 32(3). Revista Ingeniería de Construcción, 157-172. https://doi.org/10.4067/S0718-50732017000300157.*

Choque, J.; Luque, E. (2019). *Análisis estático no lineal y evaluación del desempeño sísmico de un edificio de 8 niveles diseñado con la norma E.030. Universidad Nacional de San Agustín de Arequipa.*

Cienfuegos, M. (2022). *Evaluación del desempeño estructural utilizando el análisis no lineal de la I.E. 10202 "Virgen de la Paz" - Pacora. Universidad Católica Santo Toribio de Mogrovejo*

CISMID/FIC/UNI. (s.f.). *Redes Acelerográficas en el Perú. Obtenido de http://www.cismid. uni. edu.pe/ceois/red/*

Collantes, G. (2022). *Seismic design for performance in non-structural elements using the direct displacement methodology in reinforced concrete buildings, 37(2). Revista Ingeniería de Construcción, 213-227. http://dx.doi.org/10.774/ric.00027.21.*

Comité Técnico de Normalización de Agregados, Hormigón, Hormigón Armado y Pretensado. (2001). *NTP 339.059 " Método para la obtención y ensayo de corazones diamantinos y vigas cortadas de hormigón". Lima, Perú.*

Condori, R.; Vilca, A. (2022). *Evaluación del desempeño estructural aplicando un análisis estático no lineal (Pushover) en la I. E. N.° 40230 San Antonio del Pedregal Majes - Caylloma - Arequipa. Universidad Continental.*

Cumpa, J.; Quispe, B. (2019). *Evaluación del desempeño sismorresistente de la institución educativa n°50217 de la comunidad Umachurco-San Salvador, aplicando el método de análisis estático no lineal de cedencia sucesiva (Pushover) [Universidad Andina de Cusco].https://repositorio.uandina.edu.pe/bitstream/handle/20.500.12557/2885/Brayan_Jinm y_Tesis_bachiller_2019_Part.1.pdf?sequence=1&isAllowed=y*

Department of Homeland Security Emergency Preparedness and Response Directorate FEMA Mitigation Division Washington, D.C. (2003). *FEMA-HAZUS99.Multi-hazard Loss Estimation Methodology Earthquake Model HAZUS®MH MR4 Technical Manual. Washington: Federal Emergency Management Agency.*

Díaz, D.; Diaz, S.; Pinzón, L.; Hiram, J.; Mora Ortiz, R. (2022). *Seismic performance assessment based on the interstory drift of steel, 19(2). Latin American Journal of Solids and Structures, e431.https://doi.org/10.1590/1679-78256583.*

Dirección de Normalización-INACAL. (2015). NTP 339.034 *"Método de ensayo normalizado para la determinación de la resistencia a la compresión del concreto en muestras cilíndricas". Lima, Perú.*

FEMA. Federal Emergency Management Agency. (2000). *Prestandard and Commentary for the Seismic Rehabilitation of Buildings (FEMA 356). Washington D.C.*

FEMA.Federal Emergency Management Agency. (2018). *Seismic Performance Assessment of Buildings Volume 1 – Methodology Second Edition. Washington D.C.*

Firoj, M.; Bahuguna, A.; Kanth, A.; Agrahari, R. (2022). *Effect of nonlinear soil− structure interaction and lateral stiffness on seismic performance of mid− rise RC building, (59). Journal of Building Engineering, 1-16. https://doi.org/10.1016/j.jobe.2022.105096.*

Galarza, D. (2019). *Evaluación del desempeño sísmico del edificio de la OSCUS mediante comparación del análisis estático no lineal (Pushover), análisis estático modal (Pushover multimodal) y dinámico no-lineal (historia de respuesta) [Universidad Técnica de Ambato]. https://repositorio.uta.edu.ec:8443/bitstream/123456789/29942 /1/Tesis%20I.%20C.%201334%20-%20Galarza%20Altamirano%20Daniela%20 Alexandra.pdf*

Gonzales, G.; Aguilar, A.; Huaco, G. (2020). *Incremental Dynamic Analysis of a 60 Year Old Hospital with Handmade Brick Masonry Walls. Proceedings of the LACCEI international Multi-conference for Engineering, Education and Technology, 27-31. http://dx.doi.org/10.18687/LACCEI2020.1.1.375.*

Guohua, X.; Yudong, M.; Zhaoqun, C.; Jiao, H. (2020). *Seismic Behavior of Reinforced Concrete Beam-Column Subassemblages Reinforced with Multiple Composite Central Reinforcements, 37(1). Journal of Earthquake Engineering, 58-66. https://doi.org/10. 1080 /13632469.2021.1996487.*

Huarca, B. (2022). *Análisis del desempeño sísmico no lineal estático (Pushover) en la I.E. N° 40092 "José Domingo Zuzunaga, Uchumayo – Arequipa. Universidad Cesar Vallejo.*

Jiménez, C.; Carbonel, C.; Villegas Lanza, J.; Quiroz, M.; Wang, Y. (2022). *Seismic Source of 1966 Huacho Peru Earthquake (Mw 8.1) from Tsunami Waveform Inversion. Pure and Applied Geophysics, 1-16. https://doi.org/10.1007/s00024-022-03132-7.*

Llontop, G. (2023). *Optimización del diseño estructural utilizando análisis estático no lineal Pushover en la I.E San Carlos-Monsefú [Universidad Católica Santo Toribio de Mogrovejo]. https://tesis.usat.edu.pe/bitstream/20.500.12423/6047/1/TL_LlontopMora Greta.pdf.*

Lopez, O.; Del Re Ruiz, G. (2008). *Evaluación de los métodos de análisis estático no-lineal para determinar la demanda sísmica en estructuras aporticadas de concreto armado, 46(3). IMME, 1-28.*

Lu, W.-T.; Phillips, B. (2022). *A fundamental-period-preserving seismic retrofit methodology for low-rise buildings with supplemental inerters, (266). Engineering Structures, 1-15. https://doi.org/10.1016/j.engstruct.2022.114583.*

Marín, W. (2020). *Nivel de desempeño sísmico de un edificio multifamiliar mediante el análisis estático no Lineal Pushover, Jesús María, 2020 [Universidad Cesar Vallejo]. https://repositorio.ucv.edu.pe/bitstream/handle/20.500.12692/60076/Marin_LW-SD. pdf?sequence=1&isAllowed=y*

Ministerio de Vivienda, Construcción y Saneamiento. (2006). *Norma Técnica Peruana E.020 Cargas. Lima, Perú.*

Ministerio de Vivienda, Construcción y Saneamiento. (2006). *Norma Técnica Peruana E.070 Albañilería. Lima, Perú.*

Ministerio de Vivienda, Construcción y Saneamiento. (2009). *Norma Técnica Peruana E.060 Concreto Armado. Lima, Perú.*

Ministerio de Vivienda, Construcción y Saneamiento. (2019). *Norma Técnica Peruana E.030 Diseño Sismorresistente. Lima, Perú.*

Mohammed, J. A.B.M.; Saiful, I.; Raja Rizwan , H.; Syed Danish , H. M, K. (2013). *Non-linear FEM Analysis of seismic induced pounding between neighbouring Multi-storey Structures, (10). Latin American Journal of Solids and*

Structures, 921-939. https://doi.org/10.1590/S1679-78252013000500004.

Moller, O.; Ascheri, J.; Nardi, L. (2021). *Comparison of non-linear dynamic frame response under recorded and numerically generated accelerograms, 20(3). Revista de la Construcción, 576-590. http://dx.doi.org/10.7764/rdlc.20.3.576.*

Pérez, C.; Torres, R. (2022). *Evaluación del desempeño sísmico de un edificio de muros estructurales de mediana altura en base a desplazamientos y costos de reparación probables [Universidad Católica Santo Toribio de Mogrovejo]. https://tesis.pucp.edu. pe/repositorio/bitstream/handle/20.500.12404/23901/PEREZ_NEYRA_CARLOS_EVALUACION%20_DESEMPE%c3%91O_SISMICO.pdf?sequence=1&isAllowed=y*

Pimiento, J.; Ruiz, D.; Salas, A. (2014). *Seismic performance of frames with passive energy dissipation steel slit plates, 29(3). Revista Ingeniería de Construcción, 283-298.https://doi.org/10.4067/S0718-50732014000300005.*

Reza, K.; Dadkhah, M.; Naderpour, H. (2022). *Earthquake-induced nonlinear dynamic response assessment of structures in terms of discrete wavelet transform, 39(1). Structures, 821-847. https://doi.org/10.1016/j.istruc.2022.03.060.*

Sangucho, P. (2022). *Comparación de las filosofías de diseño y el desempeño real de una estructura, mediante análisis estático lineal, análisis Pushover y análisis de historia en el tiempo en una estructura de hormigón armado, incluyendo elementos no estructurales. Escuela Politécnica Nacional.*

Seismosoft. (2020). *SeismoSignal 2020 – A computer program for signal processing of strong-motion data. Obtenido de https:// www.seismosoft.com.*

Tavera, H. (2014). *Evaluación del peligro asociado a los sismos y efectos secundarios en Perú. Lima: Biblioteca Nacional del Perú.*

Zavala, B.; Hermanns, R.; Valderrama, P.; Costa, C.; Rosado, M. (2009). *Geological process and INQUA macro-seismic intensity scale of Pisco earthquake 15/08/2007, Perú, 65(4). Revista de la Asociación Geológica Argentina, 760-779.*